Electronic Supplementary Material (ESI) for Journal of Materials Chemistry A.

Facile Sol-Gel Route to Prepare Functional Graphene Nanosheets Anchored with Homogeneous Cobalt Sulfide Nanoparticles as Superb Sodium-Ion Anodes

Tingting Chen,[a,b] Yifan Ma,[a,b] Qiubo Guo,[a,b] Mei Yang,[a,b*] and Hui Xia[a,b*]

[a.] *School of Materials Science and Engineering, Nanjing University of Science and Technology, Xiaolingwei 200, Nanjing 210094, China.*

[b.] *Herbert Gleiter Institute of Nanoscience, Nanjing University of Science and Technology, Xiaolingwei 200, Nanjing 210094, China.*

[*] Corresponding author. Tel./Fax: (86) 25 84303410. E-mail: bayberry616@njust.edu.cn (M. Yang)

[*] Corresponding author. Tel./Fax: (86) 25 84303408. E-mail: xiahui@njust.edu.cn (H. Xia)

Experimental section

Materials characterization

The physical properties of samples were characterized by X-ray diffraction (XRD, Bruker-AXS D8 Advance). Raman spectra were performed on a Renishaw inVia spectrometer with an excitation wavelength of 532 nm. The chemical state of sample on surface was investigated by X-ray photoelectron spectroscopy (XPS, ESCALAB250Xi) with a monochromatic Al anode X-ray source. The morphology and texture were investigated by field-emission scanning electron microscopy (FESEM, Quant 250FEG) and high-resolution transmission electron microscopy (HR-TEM, Tecnai G2 F30 S-TWIN). Atomic force microscopy (AFM, Bruker Veeco Multimode 8) was used to characterize the height of the sample by a tapping mode. Thermogravimetric Analysis (TGA, SDTA851E) analysis was carried out on a thermal analyzer with a heating rate of 5 °C min^{-1} from 50 to 800 °C in a flowing air atmosphere.

Electrochemical characterization

The electrode was prepared by spreading a slurry of the active material (80 wt%), carbon black (Super P) (10 wt%), and polyacrylic acid (PAA) (10 wt%) onto a Cu foil, with N-methylpyrrolidone (NMP) as the solvent. The electrode was then dried at 90 °C in a vacuum drying oven for 24 h. Electrochemical measurements were carried out using two-electrode coin cells (LIR2025) with sodium plate as both the counter and reference electrodes, and glass microfiber (Whatman, GF/F) as the separator, and 1 M $NaSO_3CF_3$ dissolved in diglyme (DGM) as the electrolyte solution. The coin cells were assembled in a glove box filled with high-purity argon. Electrochemical per of the electrodes were measured on a LAND-CT2001A instrument between 0.01 and 3.0 V vs. Na^+/Na. Cyclic voltammetry (CV) and electrochemical impedance spectroscopy (EIS) were carried out under a CHI660D electrochemical workstation. EIS measurements were performed in the frequency range from 100 kHz to 0.01 Hz at an open circuit potential by applying an AC amplitude of 5 mV. The electrochemical data were calculated based on the total mass of $Co_{1-x}S$/FGNs nanocomposites.

Table S1. Comparisons of the metal sulfide compound with different conductive matrixes for SIBs anodes from recent reported works.

Samples	Capacity (mA h g^{-1}) (cycle numbers)	ICE[a] (%) ($A\ g^{-1}$)	Capacity retention	Rate capability (mA h g^{-1}) ($A\ g^{-1}$)	Ref.
CoS/RGO	567 (1) – 231 (100)	58% (0.1)	41%	133 (2)	[1]
Co_3S_4-PNS/GS[b,c]	900 (1) – 329 (50)	53% (0.5)	37%	154 (10)	[2]
Co_3S_4@PANI[d]	550 (1) – 170 (400) 579 (1) – 253 (100)	55% (4) 70% (0.2)	31% 44%	184 (4)	[3]
cs-Co_xS_y/DPC[e,f]	600 (1) – 250 (100)	65% (0.5)	42%	110 (5)	[4]
NS-RGO-2[g]	660 (1) – 392 (50)	77% (0.1)	59%	346 (1)	[5]
Ni_3S_2-PEDOT	(1) – (50)	84%(0.6)	50%	310 (1.2)	[6]
NiSx/CNT@C	760 (1) – 380 (130)	59% (0.1)	50%	143 (5)	[7]
$Co_{1-x}S$/FGNs	493 (1) – 251 (200)	82% (1)	51%	211 (10)	This work

[a]ICE: Initial Coulombic efficiency, [b]PNS: porous nanosheet, [c]GS: graphene sheet, [d]PANI: polyaniline, [e]cs: 3-dimensional core–shell, [f]DPC: dodecahedral porous carbon, [g]NS: nickel sulfide.

The capacity retention is calculated by comparison with the discharge capacity of the 1st cycle.

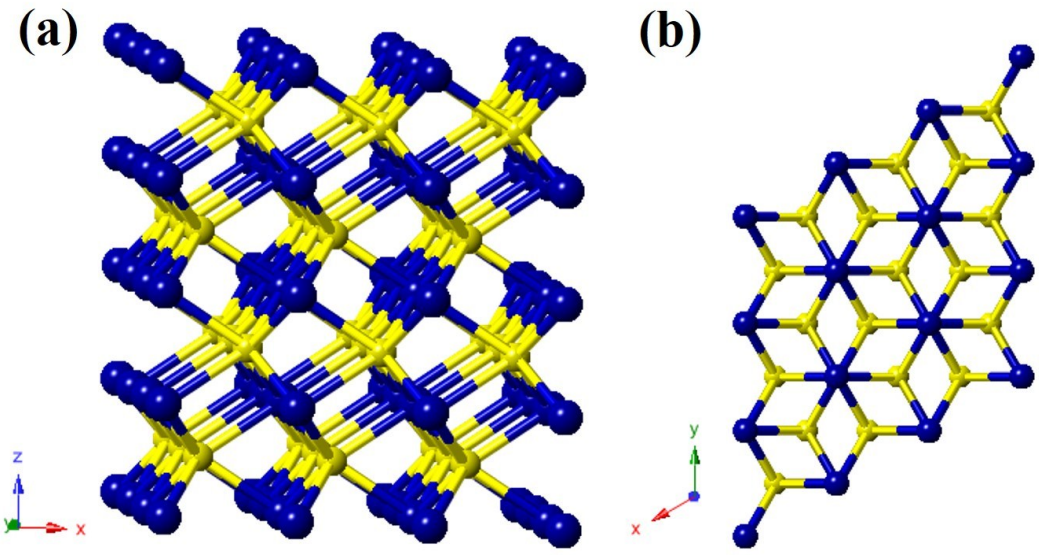

Figure S1. (a, b) Crystal structure of the stoichiometric CoS, and the $Co_{1-x}S$ prepared in this work share the same structure but with cation vacancy deficiency.

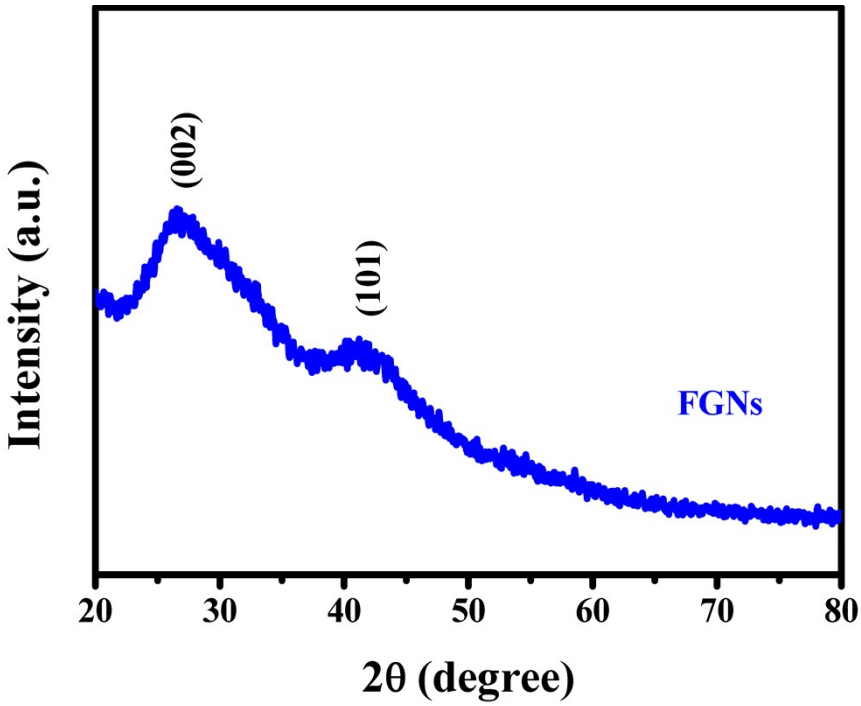

Figure S2. XRD patterns of FGNs.

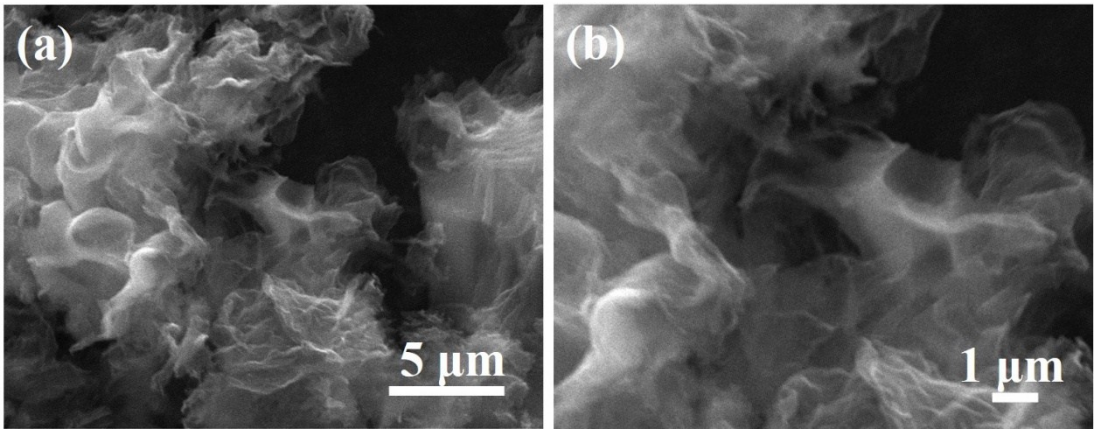

Figure S3. (a, b) SEM images of FGNs at different magnifications.

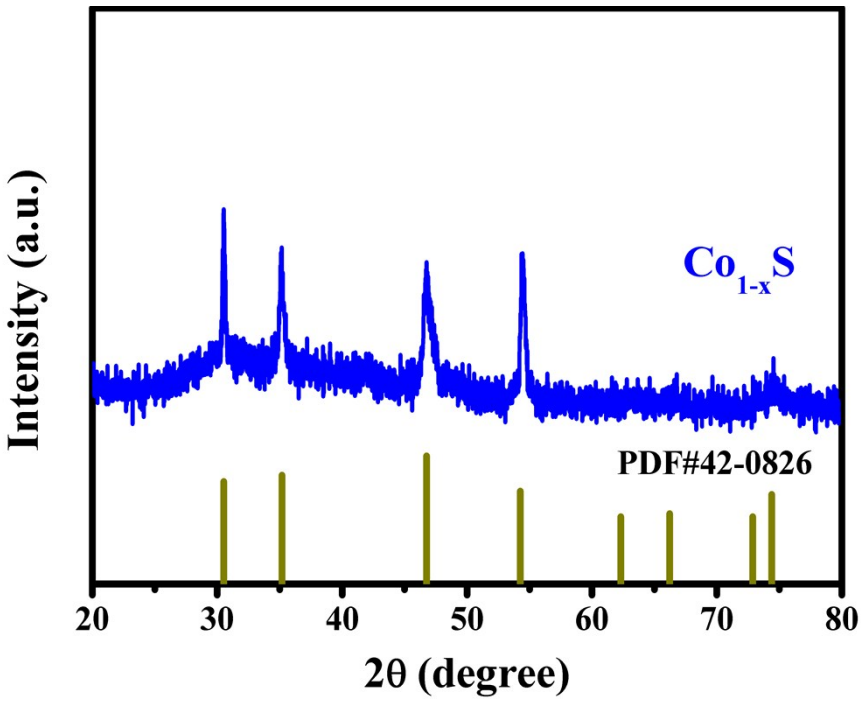

Figure S4. XRD patterns of pure $Co_{1-x}S$.

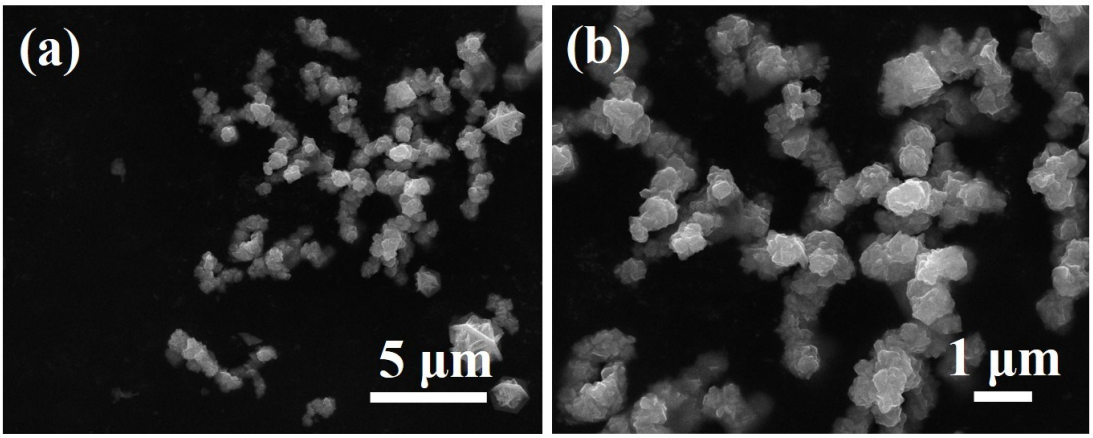

Figure S5. (a, b) SEM images of the pure phase $Co_{1-x}S$ material.

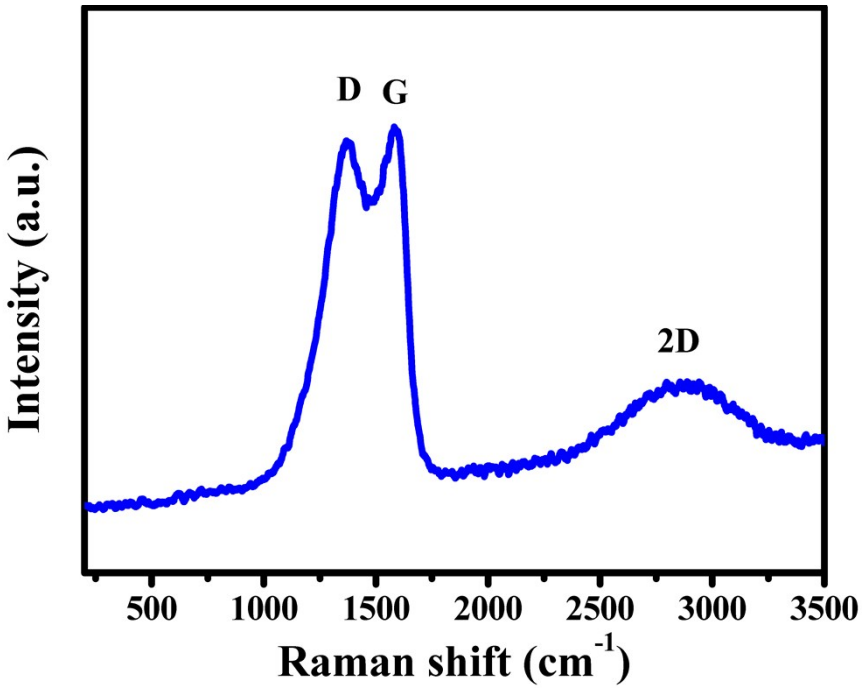

Figure S6. Raman spectra of $Co_{1-x}S$/FGNs.

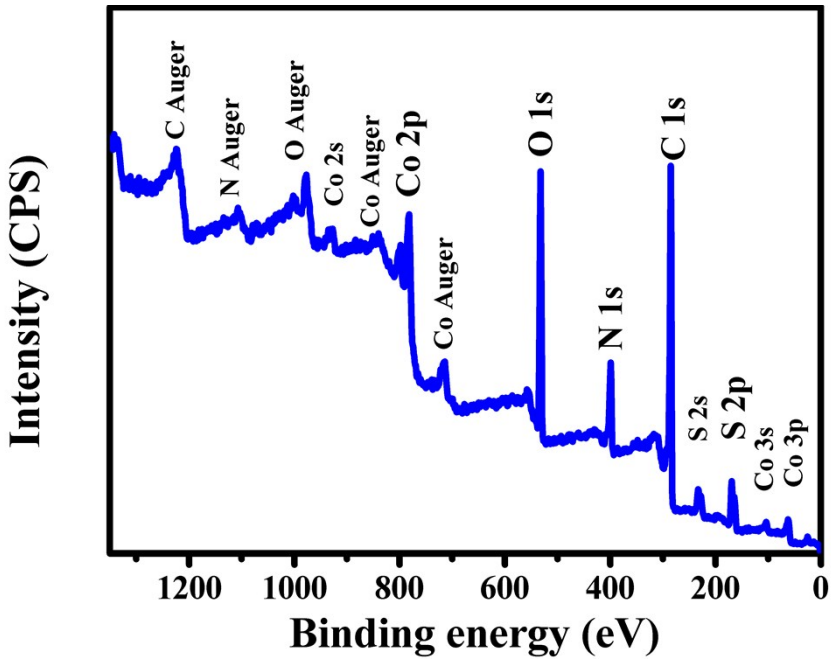

Figure S7. Wide survey of XPS spectra of $Co_{1-x}S$/FGNs.

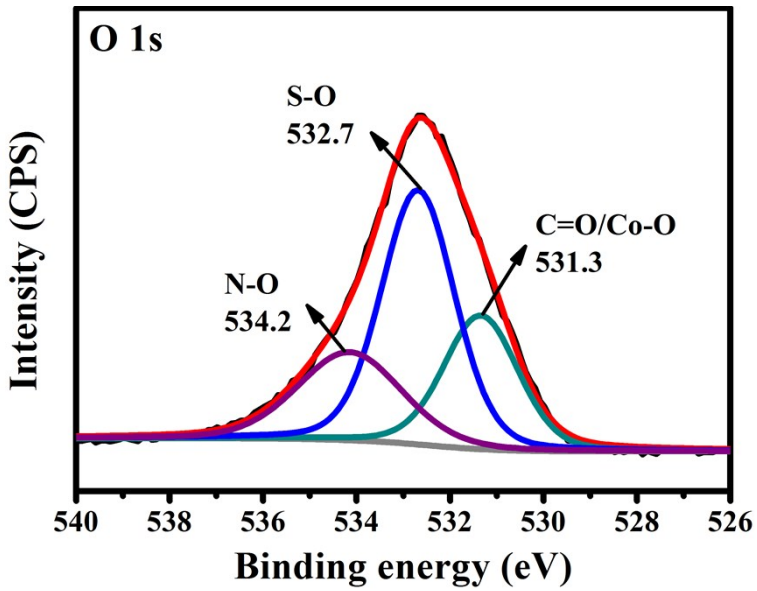

Figure S8. High resolution XPS spectra of O 1s XPS for $Co_{1-x}S$/FGNs.

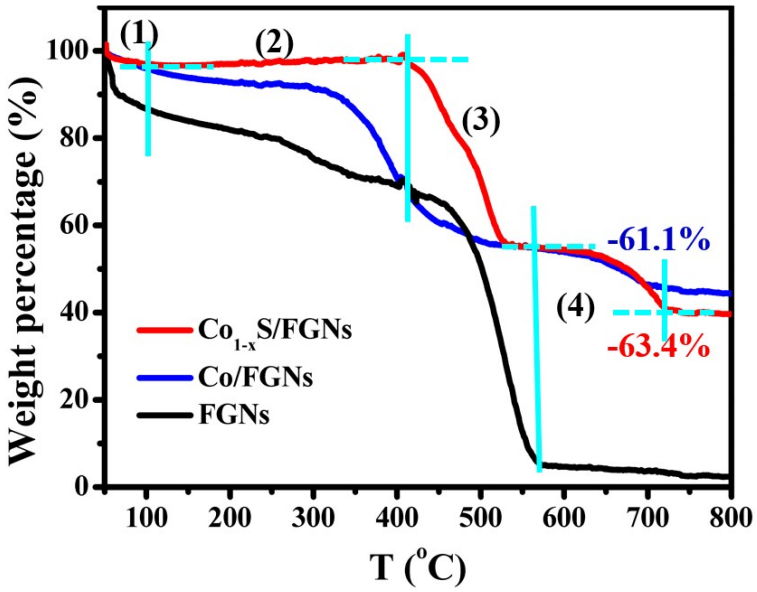

Figure S9. TGA curves of $Co_{1-x}S$/FGNs, Co/FGNs and FGNs materials.

The weight variation for $Co_{1-x}S$/FGNs sample corresponds to phase changes below: (1) the evaporation of water, (2) Partial oxidation of $Co_{1-x}S$ to $CoSO_4$ with releasing of SO_2 and oxidation of function groups in FGNs, (3) oxidation of $Co_{1-x}S$ to $CoSO_4$, Co_3O_4 and burning of carbon backbones, (4) decomposition of $CoSO_4$ to Co_3O_4.

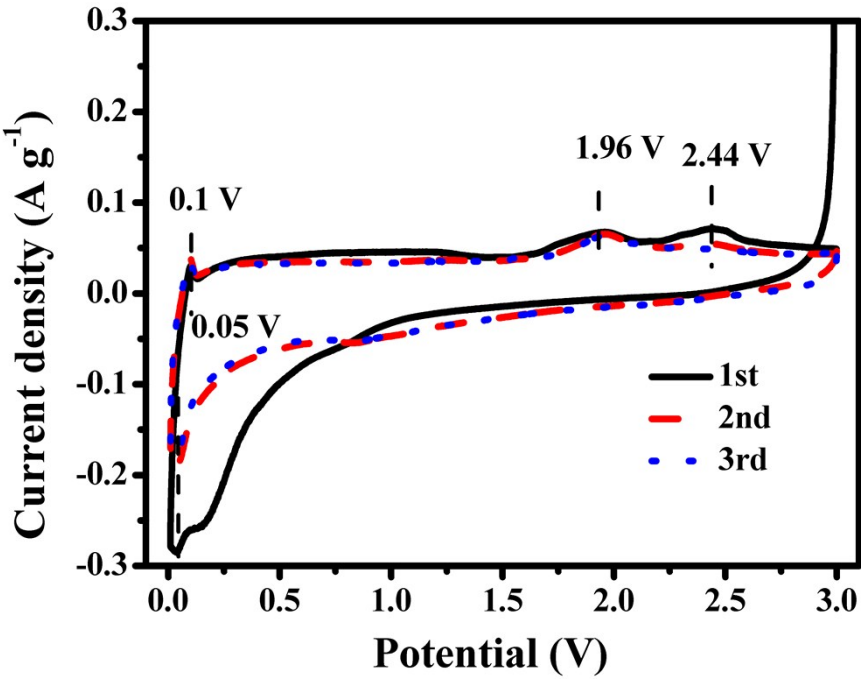

Figure S10. Cyclic voltammograms curves of the FGNs at a scan rate of 0.1 mV s^{-1}.

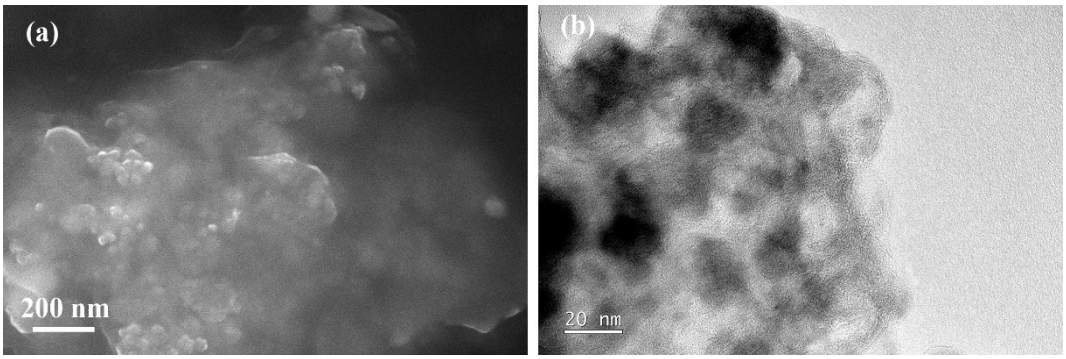

Figure S11. (a) SEM and (b) TEM images of the $Co_{1-x}S$/FGNs composites after 10 discharging/charging cycles.

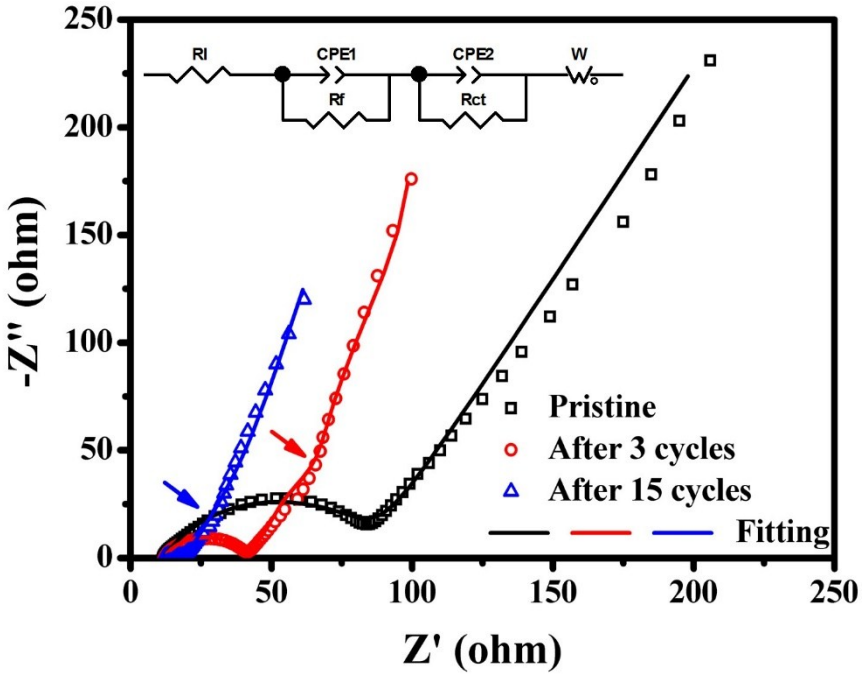

Figure S12. Electrochemical impedance spectra and equivalent circuit of the $Co_{1-x}S$/FGNs.

Table S1. R_l, R_f and R_{ct} values of $Co_{1-x}S$/FGNs nanocomposites after different cycles.

	R_l (Ω)	R_f (Ω)	R_{ct} (Ω)
Pristine	11.05	0	66.28
After 3 cycles	11.84	29.10	105.80
After 15 cycles	11.95	6.23	6.67

The R_l is internal resistance of the cell, including electric conductivity of the electrolyte, separator, and electrodes. R_f and CPE_1 are resistance and capacitance of the SEI layer formed after the first cycle. R_{ct} and CPE_2 are charge-transfer resistance and its relative double-layer capacitance. W is the Warburg impedance related to the diffusional effects of sodium ions between the active material particles and electrolyte.[8, 9]

References

1 Q. Zhou, L. Liu, G. Guo, Z. Yan, J. Tan, Z. Huang, X. Chen and X. Wang, *RSC*

Adv., 2015, **5**, 71644-71651.

2 Y. Du, X. Zhu, X. Zhou, L. Hu, Z. Dai and J. Bao, *J. Mater. Chem. A*, 2015, **3**, 6787-6791.

3 Q. Zhou, L. Liu, Z. Huang, L. Yi, X. Wang and G. Cao, *J. Mater. Chem. A*, 2016, **4**, 5505-5516.

4 Z. Zhang, Y. Gan, Y. Lai, X. Shi, W. Chen and J. Li, *RSC Adv.*, 2015, **5**, 103410-103413.

5 W. Qin, T. Chen, T. Lu, D. H. C. Chua and L. Pan, *J. Power Sources*, 2016, **302**, 202-209.

6 C. Shang, S. Dong, S. Zhang, P. Hu, C. Zhang and G. Cui, *Electrochem. Commun.*, 2015, **50**, 24-27.

7 F. Zhao, Q. Gong, B. Traynor, D. Zhang, J. Li, H. Ye, F. Chen, N. Han, Y. Wang, X. Sun and Y. Li, *Nano Research*, 2016, **9**, 3162-3170.

8 S. S. Zhang, K. Xu and T. R. Jow, *Electrochim. Acta*, 2004, **49**, 1057-1061.

9 D. Andre, M. Meiler, K. Steiner, H. Walz, T. Soczka-Guth and D. U. Sauer, *J. Power Sources*, 2011, **196**, 5349-5356.